DR. KOBAYASHI   MASAKI (Orcid ID : 0000-0002-0985-0322)

DR. TAKESHI   NAKAMURA (Orcid ID : 0000-0003-2974-6837)

WWP1 knockout in mice exacerbates obesity-related phenotypes in white adipose tissue but improves whole body glucose metabolism

Shunsuke Hoshino[1,a], Masaki Kobayashi[1,a,*], Ryoma Tagawa[1], Ryutaro Konno[1], Takuro Abe[1],

Kazuhiro Furuya[1], Kumi Miura[1], Hiroki Wakasawa[1], Naoyuki Okita[2], Yuka Sudo[1], Yuhei Mizunoe[3],

Yoshimi Nakagawa[3], Takeshi Nakamura[4], Hiroshi Kawabe[5,6,7], Yoshikazu Higami[1,*]

[1]Laboratory of Molecular Pathology and Metabolic Disease, Faculty of Pharmaceutical Sciences,

Tokyo University of Science, 2641 Yamazaki, Noda, Chiba 278-8510, Japan

[2]Division of Pathological Biochemistry, Faculty of Pharmaceutical Sciences, Sanyo-Onoda City

University, 1-1-1 Daigakudori, Sanyo-onoda, Yamaguchi, 756-0884, Japan

[3]Department of Internal Medicine (Endocrinology and Metabolism), Faculty of Medicine, University

of Tsukuba, 1-1-1 Tennodai, Tsukuba, Ibaraki, 305-8575, Japan.

[4]Division of Biosignaling, Research Institute for Biomedical Sciences, Tokyo University of Science,

2641 Yamazaki, Noda, Chiba 278-8510, Japan

[5]Department of Molecular Neurobiology, Max Planck Institute of Experimental Medicine,

 Hermann-Rein-Strasse 3, 37075 Göttingen, Germany

[6]Division of Pathogenic Signaling, Department of Biochemistry and Molecular Biology, Kobe

University Graduate School of Medicine, 1-5-6 Minatojima-minamimachi, Chuo-ku, Kobe 650-0047,

Japan

[7]Department of Gerontology, Laboratory of Molecular Life Science, Institute of Biomedical Research

and Innovation, Foundation for Biomedical Research and Innovation at Kobe, 2-2

Minatojima-minamimachi Chuo-ku, Kobe 650-0047, Japan

[a] These authors contributed equally to this work.

*Corresponding authors:

Masaki Kobayashi, PhD.

Laboratory of Molecular Pathology & Metabolic Disease, Faculty of Pharmaceutical Sciences, Tokyo

University of Science, 2641 Yamazaki, Noda, Chiba, 278-8510, Japan.

Tel/Fax: +81-4-7121-3676; Email address: kobayashim@rs.tus.ac.jp

and

Yoshikazu Higami, MD, PhD.

Laboratory of Molecular Pathology & Metabolic Disease, Faculty of Pharmaceutical Sciences, Tokyo

University of Science, 2641 Yamazaki, Noda, Chiba, 278-8510, Japan.

Tel/Fax: +81-4-7121-3676; Email address: higami@rs.noda.tus.ac.jp

Abbreviations

WAT; white adipose tissue

ROS; reactive oxygen species

TCA cycle; tricarboxylic acid cycle

WWP1; WW domain-containing E3 ubiquitin protein ligase 1

KLF2; Kruppel-like factor 2

KLF5; Kruppel-like factor 5

SPG20; spastic paraplegia 20

KO; knockout

WT; wild-type

ND; normal diet

HFD; high-fat diet

4-HNE; 4-hydroxy-2-nonenal

CBB; coomassie brilliant blue

Ppar γ ; eroxisome proliferator-activated receptor γ

Rps18; ribosomal protein S18

Sod1; superoxide dismutase 1

Sod2; superoxide dismutase 2

Trx1; thioredoxin1

Trx2; thioredoxin2

GTT; glucose tolerance test

ITT; insulin tolerance test

DTNB; 5,5-dithio-bis-(2-nitrobenzoic) acid

CS; citrate synthase

TNB; thio-bis-(2-nitrobenzoic) acid

mtDNA; mitochondrial DNA

CoxII; cytochrome c oxidase subunit II

Hprt; hypoxanthine guanine phosphoribosyl transferase

OCR; oxygen consumption rate

TGF β ; transforming growth factor β

PTEN; phosphatase and tensin homolog

Running heading

WWP1 is involved in the pathogenesis of obesity.

Abstract

White adipose tissue (WAT) is important for maintenance of homeostasis, because it stores energy

and secretes adipokines. The WAT of obese people demonstrates mitochondrial dysfunction,

accompanied by oxidative stress, which leads to insulin resistance. WW domain-containing E3

ubiquitin protein ligase 1 (WWP1) is a member of the HECT-type E3 family of ubiquitin ligases and

is associated with several diseases. Recently, we demonstrated that WWP1 is induced specifically in

the WAT of obese mice, where it protects against oxidative stress. Here, we investigated the function

of WWP1 in WAT of obese mice by analyzing the phenotype of *Wwp1* knockout (KO) mice fed a high-fat diet. The levels of oxidative stress markers were higher in obese WAT from *Wwp1* KO mice. Moreover, *Wwp1* KO mice had lower activity of citrate synthase, a mitochondrial enzyme. We also measured AKT phosphorylation in obese WAT and found lower levels in *Wwp1* KO mice. However, plasma insulin level was low and glucose level was unchanged in obese *Wwp1* KO mice. Moreover, both glucose tolerance test and insulin tolerance test were improved in obese *Wwp1* KO mice. These findings indicate that WWP1 participates in the antioxidative response and mitochondrial function in WAT, but knockdown of WWP1 improves whole-body glucose metabolism.

Keywords

white adipose tissue, obesity, WWP1, antioxidative capacity, mitochondrial function

1. Introduction

White adipose tissue (WAT) is important for maintenance of homeostasis, because it stores energy in the form of triglyceride and secretes adipokines that affect energy metabolism by modulating the activities of adiponectin, leptin, and proinflammatory cytokines. The main component of WAT is white adipocytes containing unilocular lipid droplets that hypertrophy and store excess lipid under conditions of obesity. Hypertrophy of mature adipocytes disrupts the balance in adipokine secretion, as it is accompanied by reduction in adiponectin secretion and increased release of proinflammatory cytokines that induce systemic insulin resistance, chronic inflammation, and oxidative stress [1,2].

Reactive oxygen species (ROS) are generated primarily in mitochondria and affect numerous signaling pathways [3-5]. Generally, oxidative stress is caused when the quantity of ROS generated exceeds the capacity of the antioxidant defense systems, which can result in inflammation and cell death [6,7]. Higher concentrations of ROS in WAT are closely associated with obesity-related pathologies such as hypertension, type 2 diabetes, and dyslipidemia [8,9]. Mitochondrial enzymes, which include those of the tricarboxylic acid cycle (TCA cycle), the β-oxidation process, and the electron transfer system, are important for both aerobic ATP synthesis and production of ROS. Mitochondrial dysfunction disrupts aerobic metabolism, which increases ROS production and impairs energy homeostasis. Mitochondria in WAT of obese people produce more ROS and express increased levels of markers of oxidative damage [10]. These observations indicate that oxidative stress because of increased mitochondrial ROS contributes to obesity-related pathologies.

WW domain-containing E3 ubiquitin protein ligase 1 (WWP1), also known as TIUL1 or AIP5, belongs to the HECT-type E3 ubiquitin ligase family. WWP1 has a C2 domain at its N-terminus and

four WW domains in its central region [11,12]. The C2 domain determines subcellular localization of the molecule, while the WW domains bind to proline-rich sequences (PY motif) of substrate proteins. WWP1 has been reported to be associated with various diseases. For example, WWP1 is highly expressed in high-grade breast cancer with poor prognosis [13], whereas low expression of WWP1 protein is associated with sarcopenia and abnormal neurogenesis [14-16]. Therefore, it is likely that the pathophysiologic roles of WWP1 differ between normal and cancerous tissues.

The substrates of WWP1 include Kruppel-like factor 2 (KLF2) [17], KLF5 [18,19], and spastic paraplegia 20 (SPG20) [20,21]. It is known that KLF2 and KLF5 are involved in adipocyte differentiation [18,22], while SPG20 regulates the size and number of lipid droplets [20]. Therefore, it is likely that WWP1 is involved in determining the phenotype of adipocytes.

Recently, we found that WWP1 is induced specifically in obese mouse WAT and is protective against oxidative stress in adipocytes [23]. However, we did not provide *in vivo* evidence for the roles of WWP1 in WAT. Therefore, in the present study, we explored the function of WWP1 in obese WAT and whole-body glucose metabolism by analyzing the phenotype of obese *Wwp1* knockout (KO) mice.

2. Materials and Methods

2.1. Animals

Animal experiments were approved by the Ethics Review Committee for Animal Experimentation at Tokyo University of Science (approval number: Y19054). Mice with global KO of *WWp1* (*Wwp1*$^{-/-}$ mice) and wild-type (WT) *Wwp1*$^{+/+}$ mice were generated by mating *Wwp1*$^{fl/fl}$/*Wwp2*$^{+/+}$ (*Wwp1*$^{fl/fl}$)

mice, which were obtained by crossing $Wwp1^{fl/+}/Wwp2^{fl/+}$ mice with CAG-Cre mice. $Wwp1^{fl/fl}/Wwp2^{fl/fl}$ mice were provided by Dr. Hiroshi Kawabe (Max Planck Institute of Experimental Medicine, Göttingen, Germany) [16] and CAG-Cre mice were kindly provided by Dr. Takeshi Nakamura (Research Institute for Biomedical Sciences, Tokyo University of Science, Chiba, Japan). $Wwp1^{fl/+}/Wwp2^{fl/+}$ mice were obtained by crossing $Wwp1^{fl/fl}/Wwp2^{fl/fl}$ and C57/BL6 mice. Genotyping of offspring was performed by PCR using KOD FX neo (Toyobo, Osaka, Japan) or Quick Taq® HS DyeMix (Toyobo). Primers used for genotyping were as follows: $Wwp1^{fl/fl}$ (forward, 5'-AGA GGC AAG AGA ATG GCG TCA AG-3'; reverse, 5'-CAG AAA CAG TGA TCT ACA AGT CTA AAT G-3'), $Wwp2^{fl/fl}$ (forward, 5'-GAT GGT TGT GAG CCA CTT ACT TC-3'; reverse, 5'-CCA TCA TGA ACT TCA GCC TC-3'), $Wwp1^{-/+}$ (forward, 5'-AGA GGC AAG AGA ATG GCG TCA AG-3'; reverse, 5'-GGA GGT GAA AGG GTT GGA AGA ATA C-3'), and CAG-Cre (forward, 5'-ACC TGA AGA TGT TCG CGA TTA TCT-3'; reverse, 5'-ACC GTC AGT ACG TGA GAT ATC TT-3').

  Mice were maintained under specific-pathogen-free conditions at 23°C, under a 12-h light/dark cycle in the animal facility at the Faculty of Pharmaceutical Sciences, Tokyo University of Science. They had free access to water and were fed a Charles River Formula-1 diet (21.9% crude protein, 5.4% crude fat, and 2.9% crude fiber; Oriental Yeast, Japan). At 5 weeks old, WT and KO mice were allocated to two groups: the normal diet (ND) group or high-fat diet (HFD) group. Labo MR Stock and High-Fat Diet 32 (25.5% crude protein, 32.0% crude lipid, and 2.9% crude fiber; CREA, Tokyo, Japan) were fed as the ND and HFD, respectively. At 13 weeks old, mice were euthanized under isoflurane anesthesia (Mylan, Canonsburg, PA, USA) in a fed state, and their epididymal WAT depots and liver were collected and weighed. These tissues were immediately diced, frozen in liquid nitrogen, and stored at −80°C. Blood samples were mixed with 100 mM EDTA in 1.5-ml microtubes,

centrifuged at 2,500 × g for 10 min at 4°C, and plasma was collected and stored at −80°C until analysis.

2.2. Cell lines

3T3-L1 preadipocytes were purchased from RIKEN Bioresource Center (Ibaraki, Japan). 3T3-L1/shGFP and 3T3-L1/shWwp1 preadipocytes were previously established in our laboratory using a retrovirus system [23].

2.3. Cell culture and differentiation

3T3-L1 preadipocytes were maintained in Dulbecco's-modified Eagle's medium (low glucose) (Wako) containing 10% fetal bovine serum (Thermo; Waltham, MA, USA) and 1% penicillin/streptomycin (Millipore Sigma). Differentiation of 3T3-L1 preadipocytes to adipocytes was performed as previously described [24].

2.4. Immunoblotting

Preparation of WAT lysates and immunoblotting were performed according to our previously reported methods [24]. Briefly, WAT was lysed in SDS sample buffer (50 mM tris-HCl (pH 6.8), 2% SDS, 3 M urea, 6% glycerol), boiled for 5 min, and sonicated. Lysates were subjected to SDS-PAGE (15 μg protein per well), and separated proteins were transferred to nitrocellulose membranes. Membranes were blocked with blocking solution (2.5% skim milk, 0.25% BSA in TTBS (25 mM tris-HCl pH 7.4, 140 mM NaCl, 2.5 mM KCl, 0.1% Tween 20) for 1 h at room temperature, then probed with appropriate primary antibodies overnight at 4°C. The anti-WWP1 antibody was

originally generated in our laboratory [23], anti-phospho-Akt (Ser473; #9271) and anti-Akt antibodies (#9272) were from Cell Signaling Technology (Danvers, MA, USA), and the anti-4-hydroxy-2-nonenal (4-HNE) antibody was from JaICA (MHN-020P; Shizuoka, Japan). Since the anti-4-HNE antibody nonspecifically recognizes 4-HNE-modified proteins, 4-HNE intensity was analyzed over the entire area per well on an immunoblotting membrane. Subsequently, membranes were incubated with appropriate secondary antibodies for 1 h at room temperature (horseradish peroxidase-conjugated F(ab')2 fragment of goat anti-mouse IgG or anti-rabbit IgG (Jackson Immuno Research, West Grove, PA, USA)). Antibody-bound proteins were visualized using ImmunoStar LD Reagent (Wako) and an LAS3000 Image Analyzer (Fujifilm, Tokyo, Japan), and data were analyzed using Multigauge software (GE Healthcare, Madison, WI, USA). The intensity of Coomassie Brilliant Blue (CBB) staining of membrane proteins was used to normalize target protein expression levels.

2.5. Quantitative real-time RT-PCR

Total RNA was extracted from frozen WAT using ISOGEN Ⅱ (Nippon gene, Toyama, Japan), and reverse transcription was performed using ReverTra Ace® qPCR RT Master Mix (Toyobo). Quantitative real-time PCR was performed using the CFX Connect™ Real Time System (Bio-Rad) and Thunderbird SYBR qPCR mix (Toyobo), according to manufacturer protocols. Sequences of primers used for PCR are as follows: *Adiponectin (Adipoq)* (forward, 5'-TGC CGA AGA TGA CGT TAC TAC AAC-3'; reverse, 5'-CTT CAG CTC CTG TCA TTC CAA C-3'), *Catalase* (forward, 5'-CCA AGG CAA AGG TGT TTG AG-3'; reverse, 5'-GGG TTT CTC TTC TGG CTA TGG-3'), *Leptin* (forward, 5'-CCA GGA TCA ATG ACA TTT CAC ACA C-3'; reverse, 5'-CAG GGA GCA GCT CTT GGA GAA G-3'), *Peroxiredoxin1 (Prdx1)* (forward, 5'-GCT TTC AGT GAT AGA GCC

GAT G-3'; reverse, 5'-CCA TAA TCC TGA GCA ATG GTG-3'), *Peroxisome Proliferator-Activated Receptor γ (Pparγ)* (forward, 5'-CAC AAT GCC ATC AGG TTT GG-3'; reverse, 5'-GCG GGA AGG ACT TTA TGT ATG AG-3'), *Ribosomal Protein S18 (Rps18)* (forward, 5'-TGC GAG TAC TCA ACA CCA ACA T-3'; reverse, 5'-CTT TCC TCA ACA CCA CAT GAG C-3'), *Superoxide dismutase 1 (Sod1)* (forward, 5'-GGA TGA AGA GAG GCA TGT TGG-3'; reverse, 5'-TTT GCC CAA GTC ATC TTG TTT C-3'), *Superoxide dismutase 2 (Sod2)* (forward, 5'-CCC AAA GGA GAG TTG CTG GAG-3'; reverse, 5'-CGA CCT TGC TCC TTA TTG AAG C-3'), *Thioredoxin1 (Trx1)* (forward, 5'-AGC TGA TCG AGA GCA AGG AAG-3'; reverse, 5'-ATT TTG CAA GGT CCA CAC CAC-3'), and *Thioredoxin2 (Trx2)* (forward, 5'-TTC ATG CAC AGT GGT GTG G-3'; reverse, 5'-TCA ATG GCA AGG TCT GTG TG-3'). *Rps18* was used as a housekeeping gene.

2.6. Plasma biochemical analyses

Plasma glucose, insulin, and leptin levels were measured using Autokit Glucose (Wako), a Mouse Insulin ELISA KIT (Utype) (Shibayagi, Japan), and a Quantikine® ELISA Mouse/Rat Leptin Immunoassay (R&D Systems, Minneapolis, MN, USA), respectively. All assays were performed according to manufacturer protocols.

2.7. Intraperitoneal glucose tolerance test (GTT) and insulin tolerance test (ITT)

GTT and ITT were performed using HFD-fed *Wwp1* WT and KO mice at 13–15 weeks old. Prior to GTT and ITT, mice were fasted for 24 h. D-glucose (1.0 g/kg body weight, Wako) or insulin (1.0 U/ml body weight, Wako) were injected intraperitoneally for GTT or ITT, respectively. Next, serial

blood sampling from the tail vein was performed at 0, 30, 60, and 120 min after injection. Blood glucose levels were measured using an Accu-check® aviva blood glucose meter (Roche).

2.8. Measurement of glutathione concentrations

Total glutathione (tGSH [GSH + glutathione disulfide (GSSG)]) and GSSG concentrations were measured as previously reported [25]. WAT was homogenized in extraction buffer (0.1M potassium phosphate buffer containing 5 mM EDTA (pH 7.5), 0.1% Triton X-100, and 0.6% sulfosalicylic acid) and centrifuged at 4°C for 10 min. Supernatants were used for measurement of tissue GSH content with an Infinite F200 PRO microplate reader (Tecan; Männedorf, Switzerland). The rate of 5,5-dithio-bis-(2-nitrobenzoic) acid (DTNB) formation was calculated and the concentrations of tGSH and GSSG in each sample were determined using linear regression, with reference to a standard curve. GSH concentration was calculated by subtracting GSSG concentration from tGSH concentration.

2.9. Measurement of citrate synthase (CS) activity

To prepare lysates for measurement of mitochondrial activity, WAT samples were homogenized in homogenization buffer containing 50 mM tris-HCl, pH 7.4, 150 mM NaCl, 1% phosphatase inhibitor cocktail (Thermo), 5 mM EDTA, 1% protease inhibitor cocktail (Sigma), 1% NP-40, and 0.05% sodium deoxycholate. Protein concentration in each lysate was determined using a BCA protein assay kit (Thermo Scientific; IL, USA), according to the manufacturer's protocol. CS activity was measured by monitoring color development associated with thio-bis-(2-nitrobenzoic) acid (TNB) generation from reduction of DTNB by CoA-SH, the byproduct of citrate synthesis [24]. After addition of reaction buffer, samples were incubated at 25°C for 5 min, and the reaction was initiated by addition

of 0.5 mM oxaloacetate. Changes in absorbance at 412 nm were recorded for at least 3 min using an ARVO MX/Light Wallac 1420 Multilabel/Luminescence Counter (Perkin-Elmer; MA, USA).

2.10. Measurement of mitochondrial DNA (mtDNA) content

DNA was separated and subjected to quantitative PCR using primers for *CoxII* (Cytochrome c oxidase subunit II), which is encoded by mtDNA (forward, 5'-CCA TCC CAG GCC GAC TAA-3'; reverse, 5'-AAT TTC AGA GCA TTG GCC ATA GA-3') or for *Hprt* (Hypoxanthine guanine phosphoribosyl transferase), which is encoded by genomic DNA (forward, 5'-ATC CAG GTT ACA AGG CAG CT- 3'; reverse, 5'-GGG AAA CAT AGA CAG GGG-3'). Quantitative PCR was performed using the CFX Connect™ Real Time System (Bio-Rad) and Thunderbird SYBR qPCR mix (Toyobo), according to manufacturer protocols. Relative mitochondrial copy number is represented by the amplification ratio of *CoxII* to *Hprt*.

2.11. Measurement of oxygen consumption rate (OCR)

OCR was measured as previously reported [25] in 3T3-L1/shGFP and 3T3-L1/shWwp1 cell lines after differentiation into mature adipocytes. The measurement was made using a Seahorse XF analyzer (Agilent Technologies, Santa Clara, CA, USA), according to the manufacturer's protocol.

2.12. Statistical analysis

The Tukey-Kramer test was used to analyze data, using R software (R project for Statistical Computing). Differences with *p* values <0.05 were considered statistically significant.

3. Results

Deletion of WWP1 in WAT of *Wwp1* KO mice was confirmed at the protein level (Fig. S1A). Under ND- and HFD-fed conditions, *Wwp1* KO mice showed no differences in body mass, caloric intake, or WAT mass (Fig. S1B-D).

To evaluate the levels of oxidative stress in WAT, we measured the GSH/GSSG ratio and concentration of 4-HNE adduct, which are widely used markers of oxidative stress. HFD-fed *Wwp1* KO mice had significantly higher GSSG concentrations and lower GSH/GSSG ratio than WT mice, and these differences were not observed in ND-fed mice (Fig. 1A-C). However, WAT 4-HNE adduct concentrations were similar in all groups (Fig. 1D). These results suggest that WWP1 contributes to the antioxidative response in obese WAT.

To determine whether WWP1 affects oxidative stress by influencing mitochondrial function, we measured the enzymatic activity of CS, a rate-limiting enzyme in the TCA cycle, and the level of mtDNA, a surrogate for mitochondrial content. We found that CS activity was higher in HFD-fed mice and lower in *Wwp1* KO mice than in WT mice (Fig. 2A). In contrast, *Wwp1* KO mice showed no significant differences from WT mice in mtDNA levels under both ND- and HFD-fed conditions (Fig. 2B). These results suggest that WWP1 may influence mitochondrial activity, but not mitochondrial mass, in WAT.

Obesity-induced ROS accumulation attenuates insulin signal transduction in WAT [26, 27]. To assess the effects of WWP1 on insulin signaling, we measured AKT phosphorylation (pAKT), a major intermediate of insulin signaling, and plasma glucose and insulin levels in WAT from *Wwp1* WT and KO mice. The results showed that HFD-feeding induced a significant reduction in the

pAKT/total AKT ratio, which was more marked in KO mice (Fig. 3A). Plasma insulin levels were decreased, but glucose levels were unchanged in KO mice (Fig. 3B, C). We performed GTT and ITT. Unexpectedly, both tests improved in KO mice, and WWP1 deficiency appeared to improve glucose metabolism (Fig. 3D-G).

Increased oxidative stress in adipose tissue is strongly associated with physiological processes and properties of adipocytes such as cell hypertrophy and adipokine imbalance. We examined mRNA levels of adipokines (*Adipoq* (an adipocyte differentiation marker), *Leptin*)*,* and *Pparγ*, and plasma leptin levels. Although there were no changes in *Adipoq* levels, *Leptin* levels were increased, while *Pparγ* levels were decreased in the HFD groups (Fig. 4A-C). Similarly, plasma leptin levels were increased in the HFD groups (Fig. 4D). These factors were unchanged in *Wwp1* KO mice.

4. Discussion

In the present study, we showed that WWP1 deficiency reduced the GSH/GSSG ratio because of increased concentration of GSSG in obese WAT. GSH is a tripeptide that contributes to reduction of concentrations of ROS, such as hydrogen peroxide and lipid peroxide [28]. An acute increase in ROS rapidly converts GSH to GSSG, resulting in a reduction of GSH/GSSG, without a change in total GSH. In contrast, chronic excess of ROS increases total GSH content, which increases the antioxidant capacity of tissue [29]. *Wwp1* KO mice showed normal total GSH content when fed the HFD, indicating that WWP1 may contribute to the acute antioxidative response in WAT during the early stages of obesity. This discrepancy is supported by our previously generated proteomic data, which showed that WWP1 positively regulates the expression of antioxidative proteins [23]. We also found

that 4-HNE concentrations were similar in WT and KO mice and in the ND- and HFD-fed groups. As an end-product of lipid peroxidation, 4-HNE can be considered a biomarker of chronic or cumulative oxidative stress [30]. Given the above findings, it is plausible that HFD-feeding for 8 weeks induces acute oxidative stress in WAT, but does not fully induce chronic oxidative stress, while WWP1 ameliorates the acute stress. In addition, we measured the levels of antioxidative factors, such as *Txn1/2*, *Prdx1*, *Sod1/2*, and *Catalase* (Fig. S2A-F), although they were unchanged in WAT of *Wwp1* WT and KO mice. In a recent report, we showed that antioxidant factors (e.g. TRX and PRDX) correlated with WWP1 expression according to proteome analysis *in vitro*. However, we were unable to identify any significant changes in protein expression from western blot analysis [23]. To our knowledge, the WWP1 substrates that directly contribute to the oxidative stress response have not yet been identified, although TβR1 and Smad2, WWP1 substrates involved in TGFβ (transforming growth factor β) signaling, are reported to be associated with the oxidative stress pathway [31, 32]. Therefore, a comprehensive analysis of *Wwp1* WT and KO mice is required to elucidate the mechanisms involved in the WWP1-related antioxidative response.

As described above, ROS are predominantly generated in mitochondria. CS is an important enzyme in the TCA cycle, and its activity is used as a biomarker of mitochondrial function [33]. In general, both CS activity and mitochondrial mass decrease in obesity, and CS activity correlates with mitochondrial mass. However, it has been previously reported that short-term HFD-feeding increases CS activity in skeletal muscle [34]. This finding suggests that a compensatory upregulation in mitochondrial function may occur to protect against the effects of overnutrition. The findings in skeletal muscle and the present observations regarding oxidative stress in WAT suggest that HFD increases CS activity without increasing mitochondrial mass, while WWP1 deficiency prevents full

induction of CS activity in HFD-fed mice. We also found that WWP1 knockdown reduced maximal respiration in 3T3-L1 adipocytes (Fig. S3), which was consistent with the *in vivo* data.

Several previous studies have demonstrated a relationship between oxidative stress and insulin signaling. For example, it has been shown that increased mitochondrial ROS production inhibits binding of insulin receptor substrate-1 to the insulin receptor, resulting in insulin resistance [26]. This implies that lower pAKT levels in the WAT of *Wwp1* KO mice may be attributed to cumulative oxidative stress. However, while plasma insulin levels were also lower, glucose levels were not increased in KO mice. This observation suggests WWP1 deficiency can improve glucose metabolism. Consistent with these findings, GTT and ITT suggested that WWP1 deficiency can improve whole-body glucose metabolism in obesity. It is reported that WWP1 reduces the activity of phosphatase and tensin homolog (PTEN), which inhibits AKT phosphorylation [35]. Therefore, WWP1 deficiency may inhibit PTEN suppression, resulting in reduction of pAkt in *Wwp1* KO WAT. In contrast, according to GTT and ITT, whole-body glucose metabolism was improved. Because the mice analyzed in this study did not have adipose tissue-specific KO of *Wwp1*, it cannot be ruled out that WWP1 deletion affected insulin sensitivity in tissues other than WAT (e.g. liver, skeletal muscle, and brain) and secretion of insulin from pancreatic β-cells.

In this study, the levels of *Leptin* mRNA and plasma leptin were increased in the HFD groups, but *Adipoq* mRNA levels, which are widely known to be downregulated under conditions of obesity, were unchanged. A recent study in mice with HFD-induced obesity demonstrated that a decrease in leptin levels occurs within 8 weeks of starting the HFD, whereas the decrease of adiponectin occurs over 20 weeks [36]. This report supports the validity of our results from mice fed with a HFD for 8 weeks. Increased leptin levels and decreased *Pparγ* levels are generally observed in obesity [37, 38].

However, we did not observe an effect on these factors related to *Wwp1* KO obese WAT. Therefore, we concluded that WWP1 or its related antioxidative properties exert minimal effects on adipocytes.

In our previous study, we identified WWP1 as an obesity-induced factor that positively regulates antioxidative reactions in adipocytes [23]. Consistent with these findings, in the present study, we showed that *Wwp1* KO mice exhibit lower obesity-responsive antioxidant capacity. We also showed that *Wwp1* KO mice have poorer mitochondrial function and insulin signaling capacity. Therefore, we conclude that WWP1 may be involved in maintaining WAT function, including the response to oxidative stress, mitochondrial function, and insulin signaling in obesity. Further investigation of the role of WWP1 in WAT should provide insight into obesity-related pathology in WAT. In particular, identification of the WWP1 substrates should be prioritized.

Author Contribution

M.K. and Y.H. conceived the idea, designed experiments and wrote the manuscript. S.H. predominantly performed experiments and wrote the manuscript under the leadership of M.K. and R.T. R.K., T.A., K.F., K.M. and H.W. assisted with the experiments. N.O. and Y.S. contributed to the discussion. Y.M., Y.N., T.N. and H.K. supported the experiments.

Conflict of Interest

The authors declare that they have no conflict of interest.

Acknowledgements

Supporting Documents

Fig. S1 Body mass, tissue masses, and caloric intake of *Wwp1* WT and KO mice

Fig. S2 WWP1 does not affect of mRNA expression levels of antioxidant factors in WAT.

Fig. S3 WWP1 is required for normal mitochondrial function in mature 3T3-L1 adipocytes

References

[1] Furukawa, S., Fujita, T., Shimabukuro, M., Iwaki, M., Yamada, Y., Nakajima, Y., Nakayama, O., Makishima, M., Matsuda, M., Shimomura, I. (2003) Increased oxidative stress in obesity and its impact on metabolic syndrome. J. Clin. Invest. 114, 1752-1761.

[2] Paglialunga, S., Ludzki, A., Root-McCaig, J., Holloway, G.P. (2015) In adipose tissue, increased mitochondrial emission of reactive oxygen species is important for short-term high-fat diet-induced insulin resistance in mice. Diabetologia. 58 (5). 1071-1080.

[3] Stadman, E.R., Levine, R.L. (2003) Free radical-mediated oxidation of free amino acids and amino acid resides in proteins. Amino Acids. 25. 207-218.

[4] Richter, C., Park, J.W., Ames, B.N. (1988) Normal oxidative damage to mitochondrial and

nuclear DNA is extensive. Proc. Natl. Acad. Sci. U.S.A. 85. 6465-6467.

[5] Rubbo, H., Denicola, A., Radi, R. (1994) Peroxynitrite inactivates thiol-containing enzymes of Trypanosoma cruzi energetic metabolism and inhibits cell respiration. Arch. Biochem. Biophys. 308 (1). 96-102.

[6] Sakuraba, H., Mizukami, H., Yagihashi, N., Wada, R., Hanyu, C., Yagihashi, S. (2002) Reduced beta-cell mass and expression of oxidative stress-related DNA damage in the islet of Japanese Type II diabetic patients. Diabetologia. 45 (1). 85-96.

[7] Fernández-Sánchez, A., Madrigal-Santillán, E., Bautista, M., Esquivel-Soto, J., Morales-González, A., Esquivel-Chirino, C., Durante-Montiel, I., Sánchez-Rivera, G., Valadez-Vega, C., Morales-González, J.A. (2011) Inflammation, oxidative stress, and obesity. Int. J. Mol. Sci. 12 (5). 3117-3132.

[8] Kostapanos, M.S., Spyrou, A.T., Tellis, C.C., Gazi, I.F., Tselepis, A.D., Elisaf, M., Liberopoulos, E.N. (2011) Ezetimibe treatment lowers indicators of oxidative stress in hypercholesterolemic subjects with high oxidative stress. Lipids. 46 (4). 341-348.

[9] Manna, P., Jain, S.K. (2015) Obesity, Oxidative Stress, Adipose Tissue Dysfunction, and the Associated Health Risks: Causes and Therapeutic Strategies. Metab. Syndr. Relat. Disord. 13 (10). 423-444.

[10] Chattopadhyay, M., Khemka, V.K., Chatterjee, G., Ganguly, A., Mukhopadhyay, S., Chakrabarti, S. (2015) Enhanced ROS production and oxidative damage in subcutaneous white adipose tissue mitochondria in obese and type 2 diabetes subjects. Mol. Cell Biochem. 399 (1-2). 95-103.

[11] Seo, S.R., Lallemand, F., Ferrand, N., Pessah, M., L'Hoste, S., Camonis, J., Atfi, A. (2004) The novel E3 ubiquitin ligase Tiul1 associates with TGIF to target Smad2 for degradation. EMBO J.

23 (19). 3780-3792.

[12] Zhi, X., Chen, C. (2012) WWP1: a versatile ubiquitin E3 ligase in signaling and diseases. Cell Mol. Life Sci. 69 (9). 1425-1434.

[13] Chen, C., Zhou, Z., Ross, J.S., Zhou, W., Dong, J.T. (2007) The amplified WWP1 gene is a potential molecular target in breast cancer. Int. J. Cancer. 121 (1). 80-87.

[14] Imamura, M., Nakamura, A., Mannen, H., Takeda, S. (2016) Characterization of WWP1 protein expression in skeletal muscle of muscular dystrophy chickens. J. Biochem. 159 (2). 171-179.

[15] Hirata, Y., Nomura, K., Senga, Y., Okada, Y., Kobayashi, K., Okamoto, S., Minokoshi, Y., Imamura, M., Takeda, S., Hosooka, T., Ogawa, W. (2019) Hyperglycemia induces skeletal muscle atrophy via a WWP1/KLF15 axis. J.C.I. Insight. 4 (4). e124952.

[16] Ambrozkiewicz, M.C., Schwark, M., Kishimoto-Suga, M., Borisova, E., Hori, K., Salazar-Lázaro, A., Rusanova, A., Altas, B., Piepkorn, L., Bessa, P., Schaub, T., Zhang, X., Rabe, T., Ripamonti, S., Rosário, M., Akiyama, H., Jahn, O., Kobayashi, T., Hoshino, M., Tarabykin, V., Kawabe, H. (2018) Polarity Acquisition in Cortical Neurons Is Driven by Synergistic Action of Sox9-Regulated Wwp1 and Wwp2 E3 Ubiquitin Ligases and Intronic miR-140. Neuron. 100 (5). 1097-1115.

[17] Conkright, M.D., Wani, M.A., Lingrel, J.B. (2001) Lung Krüppel-like factor contains an autoinhibitory domain that regulates its transcriptional activation by binding WWP1, an E3 ubiquitin ligase. J. Biol. Chem. 276 (31). 29299–29306.

[18] Zhang, X., Srinivasan, S.V., Lingrel, J.B. (2004) WWP1-dependent ubiquitination and degradation of the lung Kruppel-like factor KLF2. Biochem. Biophys. Res. Commun. 316 (1). 139–148.

[19] Chen, C., Sun, X., Guo, P., Dong, X.Y., Sethi, P., Cheng, X., Zhou, J., Ling, J., Simons, J.W., Lingrel, J.B., Dong, J.T. (2005) Human Krüppel-like factor 5 is a target of the E3 ubiquitin ligase WWP1 for proteolysis in epithelial cells. J. Biol. Chem. 280 (50). 41553–41561.

[20] Eastman, S.W., Yassaee, M., Bieniasz, P.D. (2009) A role for ubiquitin ligases and Spartin/SPG20 in lipid droplet turnover. J. Cell Biol. 184 (6). 881-894.

[21] Edwards, T.L., Clowes, V.E., Tsang, H.T., Connell, J.W., Sanderson, C.M., Luzio, J.P., Reid, E. (2009) Endogenous spartin (SPG20) is recruited to endosomes and lipid droplets and interacts with the ubiquitin E3 ligases AIP4 and AIP5. Biochem. J. 423 (1). 31-39.

[22] Oishi, Y., Manabe, I., Tobe, K., Ohsugi, M., Kubota, T., Fujiu, K., Maemura, K., Kubota, N., Kadowaki, T., Nagai, R. (2008) SUMOylation of Krüppel-like transcription factor 5 acts as a molecular switch in transcriptional programs of lipid metabolism involving PPAR-delta. Nat. Med. 14 (6). 656-666.

[23] Kobayashi, M., Hoshino, S., Abe, T., Okita, N., Tagawa, R., Nagai, W., Konno, R., Suzuki, Y., Furuya, K., Ishikawa, N., Okado, H., Oku, M., Iwamoto, M., Miura, Y., Sudo, Y., Higami, Y. (2019) Identification of WWP1 as an obesity-associated E3 ubiquitin ligase with a protective role against oxidative stress in adipocytes. Biochem. Biophys. Res. Commun. 508(1). 117-122.

[24] Okita, N., Hayashida, Y., Kojima, Y., Fukushima, M., Yuguchi, K., Mikami, K., Yamauchi, A., Watanabe, K., Noguchi, M., Nakamura, M., Toda, T., Higami, Y. (2012) Differential responses of white adipose tissue and brown adipose tissue to caloric restriction in rats. Mech. Ageing Dev. 133(5). 255–266.

[25] Rahman, I., Kode, A., Biswas, S.K. (2006) Assay for quantitative determination of glutathione and glutathione disulfide levels using enzymatic recycling method. Nat. Protoc. 1(6). 3159-3165.

[26] Imoto, K., Kukidome, D., Nishikawa, T., Matsuhisa, T., Sonoda, K., Fujisawa, K., Yano, M., Motoshima, H., Taguchi, T., Tsuruzoe, K., Matsumura, T., Ichijo, H., Araki, E. (2006) Impact of mitochondrial reactive oxygen species and apoptosis signal-regulating kinase 1 on insulin signaling. Diabetes 55 (5). 1197-1204.

[27] Mlinar, B., Marc, J. (2011) New insights into adipose tissue dysfunction in insulin resistance. Clin. Chem. Lab. Med. 49 (12). 1925-1935.

[28] Wu, G., Fang, Y.Z., Yang, S., Lupton, J.R., Turner, N.D. (2004) Glutathione Metabolism and Its Implications for Health. J. Nutr. 134 (3). 489-492.

[29] Asensi, M., Sastre, J., Pallardo, F.V., Lloret, A., Lehner, M., Garcia-de-la Asuncion, J., Viña, J. (1999) Ratio of reduced to oxidized glutathione as indicator of oxidative stress status and DNA damage. Methods Enzymol. 299. 267-276.

[30] Kim, C.S., Lee, S.C., Kim, Y.M., Kim, B.S., Choi, H.S., Kawada, T., Kwon, B.S., Yu, R. (2008) Visceral Fat Accumulation Induced by a High‐fat Diet Causes the Atrophy of Mesenteric Lymph Nodes in Obese Mice. Obesity. 16 (6). 1261-1269.

[31] Komuro, A., Imamura, T., Saitoh, M., Yoshida, Y., Yamori, T., Miyazono, K., Miyazawa, K. Negative regulation of transforming growth factor-beta (TGF-beta) signaling by WW domain-containing protein 1 (WWP1). Oncogene. 2004 Sep; 23(41), 6914-23.

[32] Seo, S.R., Lallemand, F., Ferrand, N., Pessah, M., L'Hoste, S., Camonis, J., Atfi, A. The novel E3 ubiquitin ligase Tiul1 associates with TGIF to target Smad2 for degradation. EMBO J. 2004 Oct; 23(19), 3780-92.

[33] Wiegand, G., Remington, S.J. (1986) Citrate synthase: structure, control, and mechanism. Annu. Rev. Biophys. Chem. 15. 97-117.

[34] Li, X., Higashida, K., Kawamura, T., Higuchi, M. (2016) Alternate-Day High-Fat Diet Induces an Increase in Mitochondrial Enzyme Activities and Protein Content in Rat Skeletal Muscle. Nutrients. 8 (4). 203.

[35] Lee, Y.R., Chen, M., Lee, J.D., Zhang, J., Lin, S.Y., Fu, T.M., Chen, H., Ishikawa, T., Chiang, S.Y., Katon, J., Zhang, Y., Shulga, Y.V., Bester, A.C., Fung, J., Monteleone, E., Wan, L., Shen, C., Hsu, C.H., Papa, A., Clohessy, J.G., Teruya-Feldstein, J., Jain, S., Wu, H., Matesic, L., Chen, R.H., Wei, W., Pandolfi, P.P. (2019) Reactivation of PTEN tumor suppressor for cancer treatment through inhibition of a MYC-WWP1 inhibitory pathway. Science. 364 (6441). eaau0159.

[36] Kwon, E.Y., Shin, S.K., Cho, Y.Y., Jung, U.J., Kim, E., Park, T., Park, J.H., Yun, J.W., McGregor, R.A., Park, Y.B., Choi, M.S. Time-course microarrays reveal early activation of the immune transcriptome and adipokine dysregulation leads to fibrosis in visceral adipose depots during diet-induced obesity. BMC Genomics. 2012. 13. 450.

[37] Lodhi, I.J., Yin, L., Jensen-Urstad, A.P., Funai, K., Coleman, T., Baird, J.H., El Ramahi, M.K., Razani, B., Song, H., Fu-Hsu, F., Turk, J., Semenkovich, C.F. Inhibiting adipose tissue lipogenesis reprograms thermogenesis and PPARγ activation to decrease diet-induced obesity. Cell Metab. 2012. 16(2). 189-201.

[38] Step, S.E., Lim, H.W., Marinis, J.M., Prokesch, A., Steger, D.J., You, S.H., Won, K.J., Lazar, M.A. Anti-diabetic rosiglitazone remodels the adipocyte transcriptome by redistributing transcription to PPARγ-driven enhancers. Genes Dev. 2014. 28(9). 1018-1028.

Figure captions

Fig. 1. WWP1 is involved in antioxidative reactions in obese WAT

(A-C) Glutathione concentrations in WAT from all groups of mice were measured spectrophotometrically at 412 nm. (A) total GSH, (B) GSSG, (C) GSH/GSSG ratio. (D) Immunoblotting of 4-HNE in WAT lysates from all groups of mice. CBB staining was used as the loading control. Quantitative values represent mean ± SD (n=3–5 per group). Differences between these values were analyzed using the Tukey-Kramer test (##, $p<0.01$ *Wwp1* WT mice (HFD-fed) *vs.* *Wwp1* KO mice (HFD-fed)).

Fig. 2 WWP1 is required for normal mitochondrial function in obese WAT

(A) CS activity in WAT from all groups of mice was measured spectrophotometrically at 412 nm. (B) Genomic *Cox2* levels were quantified using real-time PCR (n=3–5). Quantitative values represent mean ± SD. Differences between these values were analyzed using the Tukey-Kramer test (##, $p<0.01$ *Wwp1* WT mice (HFD-fed) *vs.* *Wwp1* KO mice (HFD-fed); $$, $p<0.01$ *Wwp1* WT mice (ND-fed) *vs.* *Wwp1* WT mice (HFD-fed); %%, $p<0.01$ *Wwp1* KO mice (ND-fed) *vs.* *Wwp1* KO mice (HFD-fed)).

Fig. 3 WWP1 contributes to the maintenance of insulin sensitivity in obese WAT

(A) Immunoblotting for phosphorylated AKT (pAKT) and total AKT in WAT from all groups of mice. (B, C) Plasma insulin (B) and glucose (C) levels from all groups of mice. (D-G) Blood glucose levels during GTT (D) or ITT (F) in HFD-fed *Wwp1* WT and KO mice. Each area under the curve (AUC) are calculated and shown as (E) or (G). Quantitative data represent mean ± SD (n=4–6 per

group). Differences between these values were analyzed using the Tukey-Kramer test (#, *p*<0.05, ##, *p*<0.01, ###, *p*<0.001, *Wwp1* WT mice (HFD-fed) *vs*. *Wwp1* KO mice (HFD-fed); $, *p*<0.05, $$$, *p*<0.001 *Wwp1* WT mice (ND-fed) *vs*. *Wwp1* WT mice (HFD-fed); %%%, *p*<0.001 *Wwp1* KO mice (ND-fed) *vs*. *Wwp1* KO mice (HFD-fed)).

Fig. 4 WWP1 contributes minimally to the regulation of adipokines and *Pparγ* in obese WAT

(A-C) mRNA levels of adipokines (A) *Adipoq* and (B) *Leptin*, and (C) *Pparγ* in WAT from all groups of mice were measured. (D) Plasma leptin levels from all groups of mice were measured by ELISA. Quantitative data represent mean ± SD (n=6–10 per group). Differences between these values were analyzed using the Tukey-Kramer test ($$, *p*<0.01, $$$, *p*<0.001 *Wwp1* WT mice (ND-fed) *vs*. *Wwp1* WT mice (HFD-fed); %%, *p*<0.01, %%%, *p*<0.001 *Wwp1* KO mice (ND-fed) *vs*. *Wwp1* KO mice (HFD-fed)).

A

CS activity (μmol/min μg protein)

%%

$$

##

WWP1   WT   KO   WT   KO

ND   HFD

B   mtDNA contents

Cox2 / Hprt

WWP1   WT   KO   WT   KO

ND   HFD

A

ND   HFD

WWP1   WT   KO   WT   KO

pAkt

Akt

CBB

pAkt / Akt

Relative protein levels

$

%%%

#

WWP1   WT   KO   WT   KO

ND   HFD

B

Plasma insulin levels

Insulin contents (ng / ml)

%

$$$

#

WWP1   WT   KO   WT   KO

ND   HFD

C

Plasma glucose levels

Glucose contents (mg / l)

WWP1   WT   KO   WT   KO

ND   HFD

D

GTT

— WT HFD
-- KO HFD

Plasma glucose (mg/dl)

##
##
#

Time (min)

E

##

Plasma glucose AUC (mg/dl · min)

WT   KO

HFD

F

ITT

— WT HFD
-- KO HFD

Plasma glucose (%)

##
##
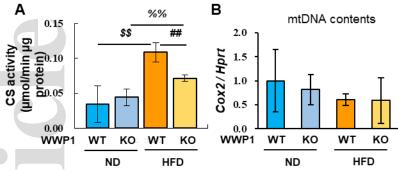
Time (min)

G

###

Plasma glucose AUC (mg/dl · min)

WT   KO
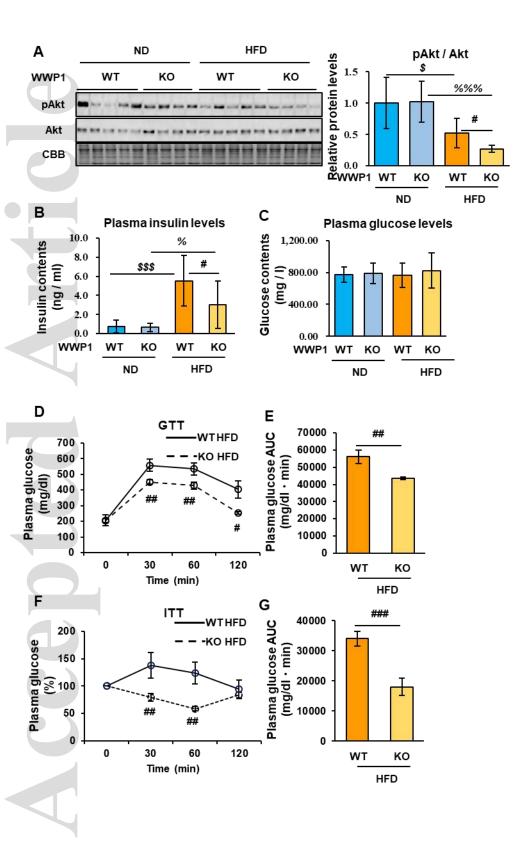
HFD

FEBS Open Bio (2020) © 2020 The Authors. Published by FEBS Press and John Wiley & Sons Ltd.

A *Adipoq / Rps18*

Relative mRNA expression

WWP1 | WT KO WT KO
ND HFD

B *Leptin / Rps18*

%%%
$$$

Relative mRNA expression

WWP1 | WT KO WT KO
ND HFD

C *Pparg / Rps18*

$$
%%

Relative mRNA expression

WWP1 | WT KO WT KO
ND HFD

D Blood leptin levels

%%%
$$$

Leptin contents (ng / ml)

WWP1 | WT KO WT KO
ND HFD